International Journal of Modern Physics B
Vol. 21, Nos. 13 & 14 (2007) 2429–2437

ALPHA-ALPHA AND ALPHA-NUCLEUS POTENTIALS: AN ENERGY-DENSITY FUNCTIONAL APPROACH

Z. F. SHEHADEH*

Physics Department, Taif Teachers College,
Taif, P.O.Box 1070, Saudi Arabia
**E-mail: z_shehadeh@yahoo.com*
www.ttc.edu.sa

A. K. BASAK, M. N. A. ABDULLAH and M. A. UDDIN

Physics Department, Rajshahi University,
Rajshahi 6205, Bangladesh

I. REICHSTEIN

School of computer Science, Carleton University,
Ottawa, Ontario K1S 5B6, Canada

M. S. SABRA and F. B. MALIK

Physics Department, Southern Illinois University,
Carbondale, Illinois 62901, USA

The real parts of the alpha-alpha and alpha-nucleus potential, particularly for ^{40,44,48}Ca and ^{58}Ni targets are determined from a realistic two-nucleon potential using an energy-density functional approach and are found to be non-monotonic with a short range repulsion in their functional forms that are similar to those needed in accounting for elastic scattering data. The deduced alpha-alpha potential has no bound states and the calculated decay width of ^{8}Be of about 6.4 eV at about 200 keV energy is in agreement with the measurement.

Keywords: Alpha-nucleus potential.

1. Introduction

Although alpha-ray was discovered over a century ago and identified to be doubly charged helium atom for nearly a hundred years[1,2], the actual nature of alpha-alpha and alpha-nucleus potential, particularly for light and medium-light nuclear targets remains incomplete. Recently, however, significant progress has been made in this direction both phenomenologically and from the fundamental aspect, relating these potentials to basic two-nucleon interaction using energy-density functional, noted henceforth as EDF, approach, by the groups of Basak in Bangladesh, Reichstein in Canada and ours in the U.S.A. In this lecture, dedicated to the celebration of the first centennial of the discovery of alpha particles, I present a gist of this endeavor.

The puzzle of alpha-nucleus potential started with the experiment of Corelli[3] *et al.* who measured unexpected large cross section, termed ALAS, of elastically scattered alpha particles by a number of nuclei, e.g. ^{28}Si, ^{32}S, which could not be analyzed by the standard optical model. This feature has subsequently been detected for many light nuclear targets as noted in ref. 4. Phenomenologically, two groups of local potentials, one proposed by Michel and his collaborators[5,6] which has a deep attractive real part having functional form of the squared Woods-Saxon potential, noted henceforth as the Michel potential, and the other by Malik and his group, a complex molecular potential with a non-monotonic real part, termed henceforth as NMS, have been reasonably successful in accounting for the data in many cases. Attempts to relate Michel potentials to two-nucleon potential in terms of folding model (FM) have met with a limited success. Quite often the potentials derived from FM need renormalization and the density distribution of alpha-particle used in folding procedure may not reproduce adequately its observed binding energy. Furthermore, in many particle-transfer reactions, e.g. ^{28,29,30}Si(α,d)^{30,31,32}P and ^{28}Si(α,p)^{31}P, the data are better accounted for by NMS potentials rather than Michel potentials in the entrance channel[7−9]. The general forms of these NMS potentials can be derived from realistic two-nucleon interactions within the context of the EDF approach outlined in the next section. In section 3, we present the results for a number of targets with a particular emphasis on alpha-alpha interaction at low energies.

2. Energy-Density Functional Theory

The EDF theory for nuclear reaction is based on the Kohn-Hohenberg theorem[10] which states that the total energy, E, of a system of interacting fermions can always be expressed as a functional of its energy-density, $\varepsilon[\rho(r)]$,

$$E = \int \varepsilon[\rho(r)]\rho(r)d^3r. \tag{1}$$

The energy density of nucleonic matter may be written as [11,12]

$$\varepsilon[\rho(r)] = T(\rho) + V_m(\rho) + V_g(\rho) + V_c(\rho). \tag{2}$$

In (2), the contribution of the kinetic energy to the energy-density, $T(\rho)$ for a nucleonic matter with Z protons and N neutrons can be calculated using the statistical theory and is given by

$$T(\rho) = (\frac{3}{5})(\frac{\hbar^2}{2M})(\frac{3\pi^2}{2})^{\frac{2}{3}}(\frac{1}{2})[(1-\alpha)^{\frac{5}{3}} + (1+\alpha)^{\frac{5}{3}}]\rho^{\frac{2}{3}}. \tag{3}$$

In (3),α is the neutron excess $(N-Z)/A$.

The mean potential,$V_m(\rho)$, generated by the mutual interaction among nucleons, i.e. the Hartree-Fock potential, can not be calculated directly from the two-nucleon interaction due to the strong short range repulsion but can be approximately obtained by evaluating the K-matrix elements using plane wave basis and is given by

$$V_n(k) = \sum_{q<k_{nf}} [(kq|K_{nn}|kq) - \text{Exchange}] + \sum_{q<k_{pf}} (kq|K_{np}|kq). \quad (4)$$

$$V_p(k) = \sum_{q<k_{pf}} [(kq|K_{pp}|kq) - \text{Exchange}] + \sum_{q<k_{nf}} (kq|K_{np}|kq). \quad (5)$$

In (4) and (5), n and p stand for neutron and proton, respectively, and k and q are wave number and momentum transfer, respectively, and f stands for Fermi-momentum. Since k is related to density, the mean nuclear potential, $V_m(\rho)$, is density dependent which can be represented as

$$V_m(\rho) = b_1(1 + a_1\alpha^2)\rho + b_2(1 + a_2\alpha^2)\rho^{\frac{4}{3}} + b_3(1 + a_3\alpha^2)\rho^{\frac{5}{3}}. \quad (6)$$

where a_i and b_i (i=1,2,3) are parameters determined by fitting the calculated energy per nucleon versus the density of nucleonic matter curve.

$V_g(\rho)$ in (3) represents inhomogenity correction to $T(\rho)$ and the nucleonic correlation energy not included in the mean field and is taken to be

$$V_g(\rho) = \eta(\frac{\hbar^2}{8M})\frac{(\nabla\rho)^2}{\rho}. \quad (7)$$

In (7), M is the nucleonic mass and the parameter η is determined by fitting the known nuclear masses with observed density distribution functions[11]. The Coulomb energy among protons with the correction due to the Pauli principle is given by

$$V_c(\rho) = 0.359(1-\alpha)\int d\acute{r}\frac{\rho(\acute{r})}{|r-\acute{r}|} - 1.0636[\frac{(1-\alpha)}{2}]\rho^{\frac{1}{3}}. \quad (8)$$

The observed nuclear masses calculated using (1) are very well reproduced with observed density distributions through proper root mean squared radii[11].

The potential between an alpha-particle and a target nucleus, $V(R)$, in the sudden approximation is given by[12]

$$V(R) = E[\rho(r,R)] - E[\rho_\alpha(r, R=\infty)] - E[\rho_T(r, R=\infty)]. \quad (9)$$

where the first term in the right hand side, RHS, represents the energy of the composite overlapped system of an alpha-particle and a target nucleus at a separation distance, R. The second and the third terms on RHS are, respectively, masses of alpha particle and target nucleus which can be taken from the observed masses or calculated using the EDF theory[11]. In the sudden approximation employed here, the density of the composite system, $\rho(r,R)$, is the sum of alpha-particle and target nuclear densities[12]

$$\rho(r) = \rho_\alpha(r) + \rho_T(r). \quad (10)$$

For target nuclei, other than alpha-particle, considered here, $\rho_T(r)$ are taken from ref. 13. The density distribution function of alpha particle, $\rho_\alpha(r)$, is reasonably represented by the following Gaussian function

$$\rho_\alpha(r) = 4(\frac{\gamma}{\pi})^{\frac{3}{2}}\exp(-\gamma r^2). \quad (11)$$

with η=7.56 fm^3 and γ=0.5, the binding energy (BE) and root mean squared radius (RMSR) of alpha-particle are, respectively, given by 19.01 MeV and 1.732 fm that are to be compared to the observed values of BE=28.3 MeV, and RMSR between 1.67 and 1.70 fm, respectively. The central density of 0.254 fm^{-3} of alpha-particle is slightly lower than 0.32 fm^{-3} needed to fit electron scattering data.

3. Results and Discussion

The main features of alpha-nucleus potentials calculated for various target nuclei up to Zr in the context of EDF theory, are that its functional form is non-monotonic and the magnitude of the attractive part is shallow, i.e., the potential is non-monotonic shallow, as the acronym NMS signifies. In fact, by slightly varying the parameters characterizing the calculated NMS potential with an imaginary part, one can usually fit the elastic scattering data well, as noted for ^{28}Si target for the first time[14]. Empirical complex NMS potentials describe very well low energy alpha-scattering data, for elastic and non-elastic processes by ^{24}Mg and ^{28}Si (ref. 8, 15). The standard form used for this empirical complex NMS potential, $V(R)$, is the following:

$$\mathrm{Re}V(r) = -V_0[1+\exp(\frac{r-R_0}{a})]^{-1} + V_1 \exp[-(\frac{r-D_1}{R_1})^2] + V_C(r). \tag{12}$$

$$\mathrm{Im}V(r) = -W_0 \exp(-\frac{r^2}{R_W^2}) - W_S \exp[-(\frac{r-D_S}{R_S})^2]. \tag{13}$$

With

$$V_C(r) = \begin{cases} (Z_1 Z_2/2R_C)(3 - r^2/R_C^2) & \text{for} \quad r \leq R_C \\ (Z_1 Z_2 e^2/r) & \text{for} \quad r > R_C \end{cases} \tag{14}$$

In the above, Z_1, Z_2, and R_C are the charges of projectile, target, and Coulomb radius, respectively. In the following, we discuss the extents to which the real parts of the empirical NMS potential in (12) (a) conform to those calculated using the EDF theory and (b) describe the elastic scattering data of alpha-particle by ^{4}He, ^{40,44,48}Ca and ^{58}Ni, noting that these have also been successful for other targets. We note here that the EDF calculations, presented here, are strictly valid for zero kinetic energy or, at energies equal to Coulomb barrier where two colliding particles have almost no kinetic energy. At much higher energies, the formalism may only serve as a guide to the general feature of the functional nature of the interaction.

3.1. $\alpha - \alpha$ *Potential*

The calculated potential of the $\alpha - \alpha$ system, shown by solid triangles in the upper insert of Fig. 1, can be well described by V_{EDF} of the functional form (12), with V_0=15.56 MeV, R_0=3.25 fm, a=0.492 fm, V_1=49.24 MeV, R_1=1.510 fm and D_1=0 fm, as well as a functional form where the first term is replaced by a Gaussian function[16]. Since non-elastic processes start well above 20 MeV excitation energies, there is no need to add an imaginary part to this potential. Except for the 5.26 MeV (lab) data, the EDF potential can generally account for the shape and magnitudes of the data at 2.0, 3.0, 8.87, 11.88 and 15.2 MeV (lab), as can be seen by comparing the calculations, noted as dashed lines, to the experimental data, shown as solid dots, in Fig. 1.

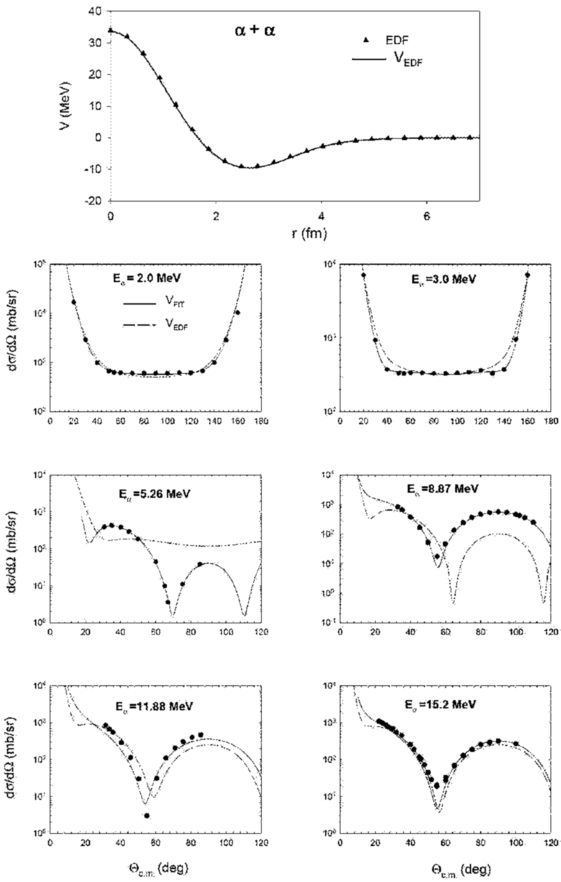

Fig. 1. EDF calculations (solid triangles) for $\alpha + \alpha$ elastic scattering are fitted, in solid line, with V_{EDF} comprising the WS attractive part and Gaussian repulsive core. The predicted cross sections using V_{EDF} (dashed lines) and those (solid lines) with the NMS potential, V_{FIT}, in Table 1, are compared to the experimental data (solid dots) at 2.0, 3.0, 5.26, 8.87, 11.88 and 15.2 MeV (lab).

The inability of the EDF potential in explaining the 5.26 MeV (lab) data points towards its failure to account for the onset of the threshold of d-wave to elastic scattering. One can, however, describe the data at all six energies by slightly changing the potential parameters, V_0 to 15.40 MeV, R_0 to 3.95 fm, a to 0.40 fm,V_1 to 150.0 MeV, and R_1 to 1.68 fm, leading to the new NMS set, V_{FIT} in Table 1.

Table 1. Comparison of the parameters of the EDF generated potential, V_{EDF}, and those of the real part of the NMS potential, V_{FIT}, needed to fit the experimental data.

Target	Set	V_0	R_0	a	V_1	R_1	D_1	R_C
^{4}He	V_{EDF}	15.56	3.25	0.492	49.24	1.51	0.00	4.00
	V_{FIT}	15.40	3.95	0.40	150.00	1.68	0.00	5.80
^{40}Ca	V_{EDF}	29.85	5.38	0.64	16.00	2.15	1.75	4.48
	V_{FIT}	31.80	5.38	0.54	18.00	2.15	1.75	6.00
^{44}Ca	V_{EDF}	29.20	5.52	0.64	15.80	2.10	1.75	4.62
	V_{FIT}	32.40	5.52	0.67	14.00	2.10	1.75	6.00
^{48}Ca	V_{EDF}	41.20	5.32	0.70	32.00	2.54	1.68	4.50
	V_{FIT}	44.00	5.32	0.70	31.70	2.54	1.68	6.00
^{58}Ni	V_{EDF}	28.50	5.92	0.668	20.00	2.30	2.15	8.50
	V_{FIT}	36.00	5.92	0.668	15.00	2.30	2.15	8.70

The fits to the data using V_{FIT} are shown as solid lines in the lower inserts of Fig. 1 and are very good. In the tail region, the two potentials are very similar, whereas they differ from each other in the interior region, mainly in the magnitudes of the repulsive part, which is primarily determined by the density function of alpha-particle near the origin. The Gaussian function (11) used in describing the alpha density does not determine the magnitude of its central part very well and hence, this repulsive part of the potential is not well described by the EDF calculation. Nevertheless, the non-monotonic nature of the $\alpha - \alpha$ potential is established and the theory determines the key part of the potential responsible in describing the low energy elastic scattering, namely, the tail region, from a realistic two-nucleon interaction, rather well. The data in this region are also well described by a simple deep monotonic potential[16,17]. However, such potentials bind two alpha particles forming ^{8}Be in s- and d-states. On the other hand, ^{8}Be is, experimentally, unbound with a decay width of (6.8±1.7) eV (ref. 18). The NMS potential deduced here does not bind ^{8}Be and has a resonance at about the right energy with a decay width of 6.36 eV, thus solving an old problem.

3.2. $\alpha-^{40,44,48}Ca$ Potential

The detailed analyses[19] of elastic scattering data by ^{40,44,48}Ca indicate that the observed data are well explained by the empirical deep monotonic Michel[5,6,20] potentials as well as NMS potentials derived from the EDF calculations. The observed density distributions of all three isotopes are described by three parameters Fermi function[13]. The BE calculated using EDF theory are, respectively, 340.44, 381.95 and 419.02 MeV for ^{40}Ca, ^{44}Ca and ^{48}Ca which are very close to the observed values of 342.06, 380.97, and 416.0 MeV, respectively. For alpha particle, γ in (11) for this case is taken to be 0.45 fm leading to a BE of 20.96 MeV, RMSR of 1.825 fm and central density of 0.217 fm^{-3}. The calculated potentials for all three targets are shown in the left insert of Fig. 2 with solid triangles. The functional form of the potential, while maintaining a NMS character, dips down near r=0 which is the consequence of the wine-bottle shape of the density distribution functions of these nuclei.

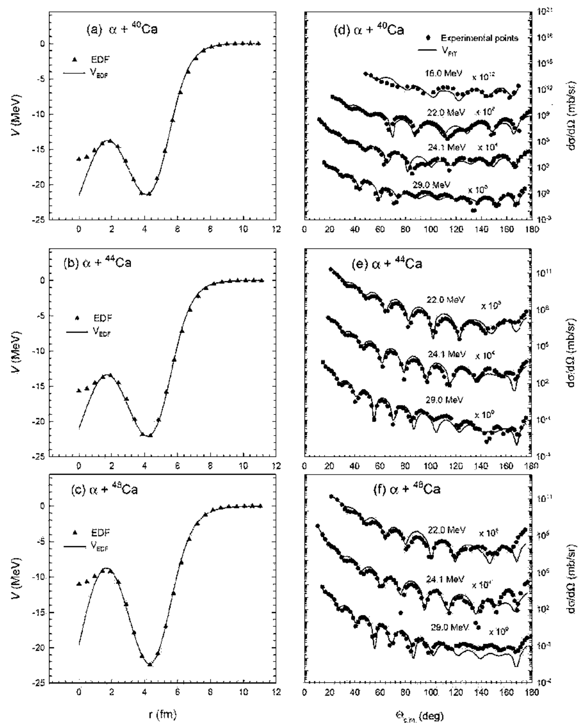

Fig. 2. Same as in Fig. 1 with the shifted Gaussian repulsive core for (a) α+^{40}Ca, (b) α+^{44}Ca and (c) α+^{48}Ca. The corresponding fits (solid lines) to the data using the V_{FIT} parameters are shown in (d), (e) and (f), respectively.

Calculated potentials are reasonably given by the parameter set, marked as V_{EDF} in Table 1, and shown as solid lines in Fig. 2. The data are reasonably reproduced by using the parameter sets, noted as V_{FIT}, in Table 1 using the imaginary components of the potential described in ref. 19. The closeness of V_{EDF} and V_{FIT} parameters in Table 1 exemplifies once again that EDF method provides a reasonable way to ascertain alpha-nucleus potential from a realistic two-nucleon interaction.

3.3. $\alpha-^{58}$*Ni Potential*

The real part of α-Ni potentials derived from the EDF theory is also reasonably close to those needed to fit the data using NMS potentials[4]. For example, the calculated potential of the alpha-^{58}Ni system, which also has a wine-bottle density distribution, is shown in the upper insert of Fig. 3, as solid triangles. Except for the interior part, this potential can reasonably be expressed by the parameters, noted in Table 1 as V_{EDF}, and is shown as solid line in the upper insert of Fig. 3. A very similar potential, the parameters of which are termed as V_{FIT} in Table 1, can reasonably account for the data between 18.0 and 50.2 MeV, as exhibited in the lower part of Fig. 3. The data for ^{60,62,64}Ni targets can similarly be described by NMS potentials, whose real parts are close to the ones derived from the EDF calculations.

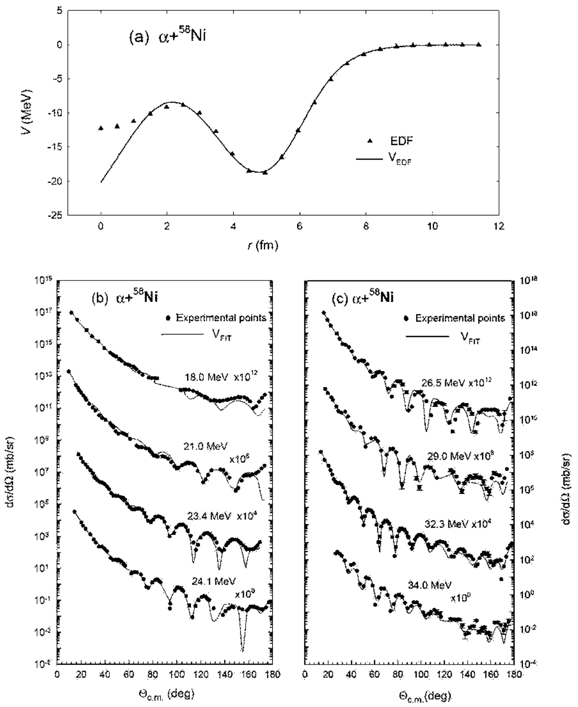

Fig. 3. Same as in Fig. 2 for α+^{58}Ni. The EDF potential (solid triangles) is fitted with the V_{EDF} set in (a). The fits to the data using the V_{FIT} set (Table 1) are shown in (b) and (c).

4. Conclusion

The examples and calculations for a number of medium light targets indicate that the general forms of real parts of alpha-nucleus potential can reasonably be derived from the realistic two-nucleon potential using the EDF method.

Acknowledgments

The authors are pleased to acknowledge the U.S. National Science Foundation grant INT-0209583 and INT-0209584 and a grant from the University Grants Commission of Bangladesh. One of the authors, FBM, is further thankful to the U.S. Army Research Office for a travel grant.

References

1. E. Rutherford, *Phil. Mag.* **11**, 166 (1906); *ibid* **12**, 134 (1906).
2. E. Rutherford and T. Royds, *Phil Mag.* **17**, 281 (1909).
3. J. C. Corelli, E. Bleuler and D. J. Tandem, *Phys. Rev.* **116**, 1184 (1958).
4. M. M. Billah, M. N. A. Abdullah, S. K. Das, M. A. Uddin, A. K. Basak, I. Reichstein, H. M. Sen Gupta and F. B. Malik, *Nucl. Phys. A* **762**, 50 (2005).
5. F. Michel, *Phys. Rev. C* **13**, 1446 (1976).
6. F. Michel and R. Vanderpoorten, *Phys. Lett. B* **82**, 183 (1978).
7. S. K. Das, A. S. B. Tariq, M. A. Uddin, A. S. Mondal, A. K. Basak, K. M. Rashid, H. M. Sen Gupta and F. B. Malik, *Phys. Rev. C* **62**, 054605 (2000).
8. S. K. Das, A. K. Basak, K. Banu, A. S. Mondal, A. S. B. Tariq, A. F. M. M. Rahman, H. M. Sen Gupta and F. B. Malik, *Phys. Rev. C* **62**, 054606 (2000).
9. S. K. Das, A. S. B. Tariq, A. F. M. M. Rahman, S. Hossain, A. K. Basak, H. M. Sen Gupta and F. B. Malik, *Phys. Rev. C* **64**, 034605 (2001).
10. P. Hohenberg and W. Kohn, *Phys. Rev.* **136**, B864 (1964).
11. M. A. Hooshyar, I. Reichstein and F. B. Malik, *Nuclear Fission and Cluster Radioactivity* (Springer Verlag 2005).
12. I. Reichstein and F. B. Malik, *Phys. Lett. B* **67**, 344 (1971).
13. H. de Vries, C. W. de Jager and C. de Vries, *Atomic Data and Nucl. Data* **36**, 495 (1987).
14. P. Manngård, M. Brenner, M. M. Alam, I. Reichstein and F.B. Malik, *Nucl. Phys. A* **504**, 130 (1989).
15. A. S. B. Tariq, A. F. M. M. Rahman, S. K. Das, A. S. Mondal, M. A. Uddin, A. K. Basak, H. M. Sen Gupta and F. B. Malik, *Phys. Rev. C* **59**, 2558 (1999).
16. M. N. A. Abdullah, M. S. Sabra, M. M. Rashid, Z. F. Shehadeh, M. M. Billah, S. K. Das, M. A. Uddin, A. K. Basak,I. Reichstein, H. M. Sen Gupta and F. B. Malik, *Nucl. Phys. A* **775**, 1 (2006).
17. B. Buck, H. Friedrich and C. Wheatley, *Nucl. Phys. A* **275**, 246 (1971).
18. J. Benn, E. B. Dally, H. H. Muller, R. E. Pixley, H. H. Staub and H. Winkler, *Phys. Lett.* **20**, 43 (1966).
19. M. N. A. Abdullah, A. B. Idris, A. S. B. Tariq, M. S. Islam, S. K. Das, M. A. Uddin, A. S. Mondal, A. K. Basak, I. Reichstein, H. M. Sen Gupta and F. B. Malik, *Nucl. Phys. A* **700**, 40 (2005).
20. F. Michel, J. Albinski, P. Belery, Th. Delbar, Gh. Grégoire, B. Tasiaux and G. Reidemeister, *Phys. Rev. C* **28**, 1904 (1983).